

OPEN ACCESS

Processing and Pretreatment Effects on Vanadium Transport in Nafion Membranes

To cite this article: Wei Xie *et al* 2016 *J. Electrochem. Soc.* **163** A5084

View the [article online](#) for updates and enhancements.



Processing and Pretreatment Effects on Vanadium Transport in Nafion Membranes

Wei Xie,^{a,b,z} Robert M. Darling,^{a,b,*} and Mike L. Perry,^{b,*}

^aJoint Center for Energy Storage Research

^bUnited Technologies Research Center, East Hartford, Connecticut 06108, USA

This work describes how manufacturing processes and pretreatments affect the proton conductivity and vanadyl permeability of Nafion[®] and how these properties are altered by running in a cell. Five Nafion membranes were examined: reinforced XL100, dispersion cast NR211 and NR212, and extruded N115 and N117. The membranes were subjected to pretreatments that included annealing at 120°C and immersing in ambient temperature and boiling water and sulfuric acid. Vanadyl permeability varied by ~15X with pretreatment and ~3X with manufacturing process. Variations in ionic conductivity were comparatively modest: ~1.5X with pretreatment and ~1.2X with processing. Differences in permeability can be eliminated by annealing the extruded membranes above their glass-transition temperature or by immersing in boiling sulfuric acid. The differences induced by processing and pretreatments were largely absent from membranes removed from vanadium redox cells subjected to repeated charge/discharge cycles.

© The Author(s) 2015. Published by ECS. This is an open access article distributed under the terms of the Creative Commons Attribution Non-Commercial No Derivatives 4.0 License (CC BY-NC-ND, <http://creativecommons.org/licenses/by-nc-nd/4.0/>), which permits non-commercial reuse, distribution, and reproduction in any medium, provided the original work is not changed in any way and is properly cited. For permission for commercial reuse, please email: oa@electrochem.org. [DOI: 10.1149/2.011601jes] All rights reserved.

Manuscript submitted July 27, 2015; revised manuscript received September 9, 2015. Published October 13, 2015. *This paper is part of the JES Focus Issue on Redox Flow Batteries—Reversible Fuel Cells.*

Perfluorosulfonic-acid (PFSA) membranes like Nafion are commonly used as separators in vanadium redox flow batteries (VRFBs) because they have high proton conductivity, low hydraulic permeability, and are stable in harsh oxidizing and corrosive environments.¹⁻³ Nafion has been widely tested in VRFBs; however, reported transport properties and cell performances vary significantly.⁴⁻¹³ One possible explanation for property differences is that thin Nafion membranes like NR212 are dispersion cast while thicker membranes like N117 are extruded.¹⁴ Another possible reason is that membranes in different studies were subjected to different treatments prior to testing, such as soaking in water^{4-6,8,9} or immersion in boiling acid.⁷ There has not been a systematic study to understand the effects of manufacturing processes and pretreatment protocols on the transport properties of Nafion membranes relevant to VRFBs, although it has been previously established that the morphology, and consequently transport properties, of Nafion are sensitive to processing conditions.¹⁵⁻¹⁸ Reinforced, cast, and extruded Nafion were subjected to various pretreatment protocols and characterized in terms of vanadyl permeability and ionic conductivity in this work to close this gap in the literature.

The concept of selectivity is widely employed in the field of membrane separations to describe performance.¹⁹⁻²² We introduce the following definition of selectivity to quantify this relationship:

$$\alpha_{V4} = \frac{\kappa RT}{F^2 P_{V4} C_{V4}} \quad [1]$$

The variables are defined as follows: α_{V4} is the dimensionless selectivity of protons over vanadyl ions VO^{2+} , κ is the conductivity in S/m, R is the universal gas constant in $\text{J} \cdot \text{mol}^{-1} \cdot \text{K}^{-1}$, T is the absolute temperature in K, F is the Faraday constant in C mol^{-1} , P_{V4} is the permeability of VO^{2+} in $\text{m}^2 \cdot \text{s}^{-1}$, and C_{V4} is the concentration of VO^{2+} in the solution adjacent to the membrane. The dimensionless selectivity can be regarded as the product of proton diffusivity and concentration divided by the product of vanadyl (VO^{2+}) diffusivity and concentration. A thin membrane with high selectivity will yield both low ohmic losses and low parasitic crossover of vanadium. Implicit in equation 1 is that diffusion is the primary mechanism of vanadium transport, which is a useful starting point especially at low current densities.²³ Although four vanadium ions V^{2+} , V^{3+} , VO^{2+} , and VO_2^+ are present in a VRFB, focusing on a single ion is sufficient

to observe trends caused by membrane treatments and exposure to the cell environment.

Interpreting the magnitude of the selectivity is not intuitive. However the selectivity can be related to the energy efficiency of a flow battery. One can show that the maximum energy efficiency of a flow battery depends on selectivity (see Appendix, the subscript V4 has been dropped):

$$\varepsilon_{e,rt} = \left(1 - \sqrt{\frac{\phi RT (1 + \tau) (1 + \tau^{-1})}{\alpha F U}} \right)^2 \quad [2]$$

This expression can be used to calculate the maximum efficiency of a flow battery as a function of temperature T , ratio of charge to discharge times τ , selectivity of the limiting component α , and open-circuit potential U ; provided the area-specific resistance is dominated by the membrane (if this is not the case, then divide α by $1 + R_0 \kappa / l$, where R_0 is the sum of other contributions to the area-specific resistance and l is the thickness of the membrane). The proportionality constant ϕ depends on the reactions associated with crossover and the charge carried by the particular species for which α is defined, V4 in this case. For a VRFB with equal fluxes of all vanadium species across the membrane $\phi = 4$.²³ Equation 2 applies when polarization is linear and parasitic crossover occurs by diffusion. Interestingly the maximum efficiency is independent of membrane thickness when $R_0 = 0$. The energy inefficiency, $1 - \varepsilon_{e,rt}$, which is easier to compare when the efficiency is near 100% as used in this work.

Experimental

Membrane treatment.— Commercial Nafion membranes were purchased from *Ion Power Inc.* (DE, USA). XL100 is a thin, fiber-reinforced membrane (~25 μm), NR211 and NR212 are dispersion cast, and N115 and N117 are extruded.¹⁴ Vanadyl sulfate (VOSO_4 , 99.9%) and magnesium sulfate (MgSO_4 , anhydrous, >99.5%) were purchased from *Alfa Aesar* (MA, USA). Sulfuric acid (H_2SO_4 , 95.0–98.0 w/w %) was purchased from *Fisher Scientific* (PA, USA). The VOSO_4 solutions were filtered before use. Other chemicals were used as received. Pretreatment methods are described in Table I. All membranes were tested immediately after pretreatment.

Water uptake.— Water uptake was measured by soaking Nafion membranes in de-ionized water at ambient conditions for at least

*Electrochemical Society Active Member.

^zE-mail: xiew@utrc.utc.com

Table I. Nomenclature and brief description of membrane pretreatments.

Nomenclature	Pretreatment
As received	Used without any treatment
Water treated	Soaked in deionized (DI) water for 3 days
Electrolyte treated	Soaked in 1.5 M VOSO ₄ / 2.6 M H ₂ SO ₄ solution for 3 days
Boiled	Boiled in 0.5 M H ₂ SO ₄ solution for 2 hours and then in DI water for 2 hours
Heat treated	Heated in an oven at 120°C for 3 days in air

3 days. The hydrated membranes were periodically weighed until a constant wet mass (m_h) was obtained. Lint-free tissue paper was used to wipe the membrane surface to remove water droplets before weighing. Then, the hydrated membranes were dried under vacuum at 110°C for at least 2 days. Samples were periodically weighed until a constant dry mass (m_d) was obtained. The equilibrium volume fraction of water in the hydrated membranes (ϕ_w) was calculated as follows:

$$\phi_w = \frac{(m_h - m_d) / \rho_w}{(m_h - m_d) / \rho_w + m_d / \rho_p} \quad [3]$$

where ρ_p is the density of dry membrane and ρ_w is the density of water, 1.0 g/cm³. The density of dry Nafion was taken as 2 g/cm³ based on literature.²⁴

Ionic conductivity.— Ionic conductivity was measured in a Fuel Cell Test System (Series 890B, Scribner Associates Inc., NC, USA) by impedance spectroscopy using a Solartron 1255B Frequency Response Analyzer coupled with a Solartron SI 1287 Electrochemical Interface. The impedance was recorded in the frequency range from 1 MHz to 1 Hz with a perturbation current amplitude of 0.5 mA. The membrane was embedded in a four-point-probe conductivity cell (BekkTech #BT-112, BekkTech LLC, CO, USA) with platinum mesh. Droplets on the surface of treated membranes were wiped off with tissue paper before assembly. A fully-humidified mixture of 4 vol.% hydrogen in nitrogen was purged through the cell at a flow rate of 0.25 L/min to control humidity. Measurements were conducted at 25°C and 100% relative humidity after equilibrating for 2 h. The ionic conductivity, κ , was calculated as follows:

$$\kappa = \frac{l}{RS} \quad [4]$$

where l is the distance between the two central probes of the conductivity cell, S is the area of a membrane cross section, and R is the resistance calculated with ZPlot and ZView software (Scribner Associates Inc., NC, USA).

Vanadyl permeability.— Vanadyl permeability was measured using a dual-chamber, direct-permeation cell (Side-Bi-Side Cells, PermeGear Inc., PA, USA) by a method similar to that described in the literature.^{19,25} The membrane was clamped between the two chambers to prevent leaks. The volume, V , of solution added to each chamber was 45 mL, and the area available for mass transport (defined by the circular openings of the permeation cell) was 1.77 cm². The donor chamber was initially filled with a solution containing 1.5 M VOSO₄ and 2.6 M H₂SO₄, and the receiver chamber was initially filled with a solution containing 1.5 M MgSO₄ and 2.6 M H₂SO₄. These solutions have equal ionic strengths which minimizes differences in osmotic pressure. The temperature was maintained at 25°C by water circulating through the outer jacket of the permeation cell. A magnetic stir bar was placed in each chamber to ensure good mixing of the solutions. Samples (5 mL each) were taken at regular time intervals from the receiver chamber to determine vanadium concentration, and 5 mL of 1.5 M MgSO₄/2.6 M H₂SO₄ solution was added to the receiver chamber after sampling to maintain a constant solution volume. The

vanadium concentration was measured using a Gary 5000 UV-vis-NIR spectrometer (Varian Inc., CA, USA). The characteristic absorption of VOSO₄ in UV-vis analysis was selected at the wavelength of 248 nm. The vanadium concentration in the receiver cell was less than 10 mM in all cases, and the UV-Vis response was linear within this concentration range at 248 nm. Within this low concentration range we found the absorption at 248 nm to be more sensitive than the response obtained at 700–750 nm, which is the wavelength commonly used for higher concentrations.

Applying Fick's First Law of diffusion²⁶ and material balances on both chambers, vanadyl permeability, P , can be defined as follows:²⁷

$$\begin{aligned} V \frac{d c_R(t)}{d t} &= P \frac{A}{d} [c_D(t) - c_R(t)] = P \frac{A}{d} [(c_D(0) - c_R(t)) - c_R(t)] \\ &\approx P \frac{A}{d} [c_D(0) - c_R(t)] \end{aligned} \quad [5]$$

where $c_R(t)$ is the vanadyl concentration at time t in the receiver chamber, and $c_D(0)$ is the initial vanadyl concentration in the donor chamber. Equation 5 applies when the concentration profiles in the membrane are fully developed. The approximate form on the right is arrived at by ignoring concentration changes in the donor chamber and is frequently applied in the literature.^{5,9,28} The exact version of Equation 5 can be integrated to give:

$$P = -\frac{Vd}{At} \ln \left(1 - 2 \cdot \frac{c_R(t)}{c_D(0)} \right) \quad [6]$$

The vanadyl permeability was calculated using Equation 6 in this study. The permeability differs from the diffusion coefficient primarily because it is based on the concentrations in the bulk solutions adjacent to the membrane, not the concentrations in the membrane.

VRFB cell testing.— VRFB cell testing was done with electrolyte solutions containing 1.5 M vanadium (VOSO₄ hydrate, Alfa Aesar, 99.9% on a metals basis) and 4.1 M total sulfate (Fisher-Scientific 95–98% H₂SO₄, diluted with de-ionized water). The positive and negative electrolytes were prepared by charging solutions initially consisting of VOSO₄ (VO²⁺ denoted V4) in H₂SO₄. The first charge yields V³⁺ (V3) and VO₂⁺ (V5). The positive solution was then discarded and replaced with VOSO₄ and the cell was then charged again to yield V²⁺ (V2) and V5. The masses of the positive and negative electrolytes after all preparatory steps were 90 g and 100 g, respectively. The electrolytes were fed to the cell at 120 ml/min with peristaltic pumps. Temperature was not controlled, and was approximately 20°C. Both storage vessels were purged with nitrogen. Each cell had interdigitated flow fields on both sides, and an active area of 23 cm². All cells contained identical carbon-paper electrodes that were heat treated in air at 400°C for 30 h in order to increase catalytic activity. The heat-treatment resulted in approximately 1.5% mass loss. The areal specific mass of carbon was between 12 and 14 mg/cm² on both sides. Cells were cycled between 0.7 V and 1.65 V at several current densities using a battery tester from Arbin Instruments. All cell tests lasted about ~200 h.

Results and Discussion

This section begins with a summary of permeability and conductivity measurements on cast, extruded, and reinforced Nafion membranes subjected to the five treatments listed in Table I. The selectivities and associated energy inefficiencies calculated from these values are then presented and discussed. This is followed by an examination of how transport properties were altered by operation in a cell. The transport properties of membranes were measured before and after charge/discharge cycling in a cell. Finally the impact of lengthy immersive treatments on permeability is examined to distinguish the effects of cycles from the effects of time.

Permeability and conductivity of membranes after various pretreatments.— The permeabilities of vanadium through the five different Nafion membranes subjected to the five pretreatments in

Table II. Vanadyl permeability of different Nafion membranes with various pretreatments.

Membrane	Vanadyl Permeability $\times 10^7$ (cm ² /min), 25°C					
	Heat treated	As received	Electrolyte treated	Water treated	Boiled	Max./Min.
XL100	1.29*	1.29 ± 0.05	1.45	4.19	25.7	19.9
NR211	1.89*	1.89 ± 0.07	2.04	5.95	23.8	12.6
NR212	1.59 ± 0.07	1.53 ± 0.09	1.79 ± 0.08	5.40 ± 0.32	27.9 ± 3.3	18.2
N115	1.58	4.35 ± 0.09	4.52	6.68	23.8	15.1
N117	1.53	4.13 ± 0.08	4.37	7.70	25.9	16.9
Max./Min.	1.5	3.4	3.1	1.8	1.2	

*Estimated from as-received samples by assuming that heat-treatment did not alter membrane properties, which is consistent with the results for NR212.

Table I are shown in Table II; errors are included when the measurements were repeated. Repeated measurements were deemed unnecessary for all samples, since the errors were sufficiently small in the samples that were repeated. The results are colored red, yellow, or green based on magnitude, with green being the best or lowest. The final row gives ratios of maximal to minimal permeability for different membranes subjected to the same treatment. Similarly, the final column gives ratios of maximal to minimal permeability for the same membrane subjected to different treatments. Permeability varies by a factor of 12.6 to 19.9 with pretreatment and 1.2 to 3.4 with manufacturing process. The permeabilities of all of the membranes are similar and low after heat-treatment, and similar and high after immersion in boiling sulfuric acid and water. The extruded membranes have consistently higher permeabilities than the cast membranes when subjected to the other three treatments. The difference is largest in the as-received state, smaller after soaking in electrolyte, and smallest after soaking in water.

Water uptake was measured for the as-received and boiled membranes and volume fractions of water in the hydrated membranes are shown in Table III as an indicator of fractional free volume in the swollen polymer matrix. Water molecules serve as plasticizers in PFSA membranes because they enlarge the free volume within the polymer matrix, which is evident from the large amount of swelling that occurs when these membranes are equilibrated with aqueous solutions.^{2,29} This increase in free volume increases salt permeability.^{30,31} Immersing the membranes in boiling sulfuric acid results in additional swelling, since the plasticized membrane is also subjected to a temperature close to the glass-transition temperature of dry Nafion ionomer (110 to 120°C³²). This pretreatment effectively overwrites the thermal history of the membranes, and leads to the opening of large continuous hydrophilic pathways, which were previously isolated free-volume voids connected by tiny channels.¹⁸ The order-of-magnitude increase in vanadyl permeability of the boiled membranes occurs because the transport of salts through these membranes is taking place within a free volume and morphology that is substantially altered relative to the as-received membranes.¹⁶

Table III. Volume fraction of water in hydrated Nafion membranes.

Membrane	Volume Fraction of Water (%)	
	As received	Boiled
XL100	27.4 ± 0.9	55.9 ± 2.8
NR211	33.1 ± 1.5	59.8 ± 3.6
NR212	31.4 ± 1.2	54.8 ± 3.1
N115	41.9 ± 1.8	52.1 ± 3.3
N117	40.7 ± 1.5	53.8 ± 2.7
Max./Min.	1.53	1.15

N115 is manufactured by extrusion and quenching at ambient conditions, which should result in a high degree of amorphous structure.³³ This morphology has a larger fractional free volume, which presumably explains the high permeability of the as-received N115 compared to as-received cast membranes. A heat-treatment conducted close to the glass-transition temperature of the ionomer acts as an annealing process during which the polymer matrix is reoriented and crystallinity increases. This reorientation leads to a reduction in the free volume,¹⁷ which results in decreased vanadium permeability. Substantial changes were not observed with NR212, because the dispersion-casting manufacturing process involves drying at high temperature that result in a less amorphous polymer matrix, which is similar to the polymer after thermal treatment. Heat treating NR212 and N115 for 10 days (not shown) gave substantially the same results as heat treating for 3 days. Furthermore, heat treating NR212 and N115 after either soaking in water or boiling solutions (not shown) gave permeabilities matching the heat-treated values shown in the second column of Table II.

Table IV reports the ionic conductivities of the different Nafion samples. The table has the same format as Table II, with green indicating high conductivity. Clearly, the conductivity varies less with both treatment and manufacturing process than vanadyl permeability. The substantial morphology differences induced by processing have less impact on proton movement than vanadyl movement. The conductivity, like the permeability, is more sensitive to pretreatment than manufacturing process. The ranking of the conductivities is nearly the inverse to the ranking of permeabilities, which is not surprising given that the conductivity is proportional to the diffusion coefficient of protons, and high conductivity is favorable while high vanadyl permeability is unfavorable.

Table V shows selectivities calculated for the different membranes. The selectivities can be divided into the same three categories as the permeabilities as indicated by the coloring. Comparing the variability of ionic conductivity and vanadyl permeability, it is readily apparent that the variability of the selectivity is dominated by vanadyl permeability. Selectivity varies > 10X for treatment and < 3X for manufacturing. The selectivities of all membranes are best and similar after heat treatment; and worst and similar after immersion in boiling sulfuric acid. Thus, both of these treatments eliminate differences caused by manufacturing, but heat-treatment gives 10X better selectivity. The dispersion-cast membranes are better than the extruded membranes in the as-received state and this order continues after treatment in room temperature electrolyte. Exposure to room temperature water causes the selectivities to worsen and the distinction between cast and extruded membranes to diminish.

Table VI shows the minimum energy inefficiencies for hypothetical VRFB cells having the selectivities in Table V, $\tau = 1$, and $\phi = 4$. The minimum inefficiency ranges from 1.5% to 5.6%. The heat treated samples would be the most efficient while the boiled samples would be the least efficient, if these properties remained stable during operation in a VRFB cell.

Table IV. Ionic conductivity of different Nafion membranes with various pretreatments.

Membrane	In-plane Ionic Conductivity (mS/cm), 25°C, RH=100%					
	Heat-treated	As received	Electrolyte-treated	Water-treated	Boiled	Max./Min.
XL100	58.8*	58.8 ± 3.3	54.2	67.8	86.1	1.6
NR211	69.7*	69.7 ± 3.8	62.1	78.5	87.9	1.4
NR212	68.9 ± 2.2	67.6 ± 1.6	64.9 ± 1.8	82.4 ± 4.6	93.7 ± 7.1	1.4
N115	58.4	71.0 ± 3.4	65.0	84.0	86.7	1.5
N117	60.2	67.8 ± 2.8	64.3	79.3	92.1	1.5
Max./Min.	1.2	1.2	1.2	1.2	1.1	

*Estimated from as-received samples by assuming that heat-treatment did not alter membrane properties, which is consistent with the results for NR212.

Table V. Selectivities of different Nafion membranes subjected to various pretreatments.

Membrane	Selectivity (dimensionless)					
	Heat treated	As received	Electrolyte treated	Water treated	Boiled	Max./Min.
XL100	4855	4855	3981	1723	357	14
NR211	3928	3928	3242	1405	393	10
NR212	4615	4706	3862	1625	358	13
N115	3937	1738	1532	1339	388	10
N117	4191	1748	1567	1097	379	11
Max./Min.	1.2	2.8	2.6	1.6	1.1	

Table VI. Minimum energy inefficiencies of VRFBs with selectivities in Table V.

Membrane	Minimum Energy Inefficiency (%)					
	Heat treated	As received	Electrolyte treated	Water treated	Boiled	Max./Min.
XL100	1.5	1.5	1.7	2.6	5.6	36
NR211	1.7	1.7	1.9	2.9	5.4	3.1
NR212	1.6	1.6	1.7	2.7	5.6	3.6
N115	1.7	2.6	2.7	2.9	5.4	3.2
N117	1.7	2.6	2.7	3.2	5.5	3.3
Max./Min.	1.1	1.7	1.6	1.3	1.0	

Figure 1 shows the selectivity of heat-treated, as-received, and boiled NR212 and N115 before and after charge/discharge cycling in a VRFB cell. Table VII contains the selectivities in Figure 1, as well as the measured permeabilities and conductivities. During cell testing, the membranes with different pretreatments were subject to the same conditions including clamping pressure, temperature, water activity, electrolyte composition, and current density. The differences between the samples associated with the pretreatments were dramatically reduced after cycling in a cell. The selectivity of the heat-treated and as-received membranes decreased while the selectivity of the membranes immersed in boiling sulfuric acid increased. Selectivity appears to approach a common value of approximately 1200 (the dashed-purple line) regardless of pretreatment and manufacturing process. A selectivity of 1200 corresponds to a maximum energy efficiency of ~97% for $\tau = 1$, $R_{\Omega} = R_m$, and $U = 1.42$ V. The NR212 selectivities are more tightly grouped than the N115 after the cell test. Perhaps NR212 responds more quickly to the cell environment because it is thinner than N115. The selectivities of NR212 and N115 after immersion in water are shown by the horizontal lines, which are above the proposed ultimate value. While one might expect the selectivities of membranes subjected to charge/discharge cycling in a cell to approach the selectivities of membranes soaked in electrolyte as seen in Table V, they are in fact lower than the selectivities of the membranes soaked in water, which are in turn lower than the selectivities of membranes soaked in electrolyte. One possibility explored in the next section is

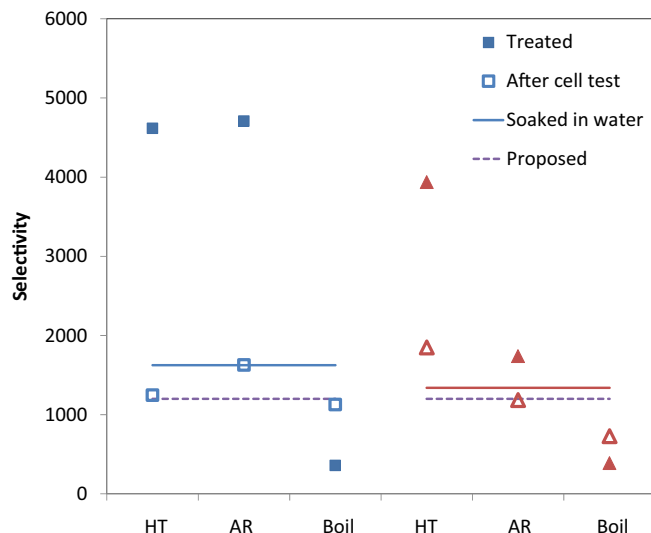


Figure 1. A comparison of selectivity before and after cycling in a VRFB cell. Squares denote NR212; triangles denote N115. Filled symbols denote before test, while open symbols denote after cell test. The solid horizontal lines are the selectivities of NR212 and N115 after immersion in water from Table V.

Table VII. Selectivity, permeability, and conductivity before and after cycling in a VRFB cell.

Membrane	Treatment	Selectivity		Permeability ($\times 10^7$ cm ² /min)		Conductivity (mS/cm)	
		Treated	Post cell	Treated	Post cell	Treated	Post cell
NR212	Heat treated	4615	1246	1.59	5.11	68.9	59.7
	As received	4706	1627	1.51	4.17	67.6	63.6
	Boiled	358	1127	31.2	6.37	128	80.8
	Max./Min.	11	1.3	20	1.5	1.9	1.4
N115	Heat treated	3937	1849	1.58	3.17	58.4	55.2
	As received	1738	1185	4.35	6.01	71.0	67.5
	Boiled	388	729	23.8	7.69	86.7	71.1
	Max./Min.	7.5	1.9	15	2.4	1.5	1.3

that the membranes immersed in water and electrolyte did not have sufficient time to reach equilibrium.

Effect of soaking time.— Figure 1 suggests that subjecting membranes to charge/discharge cycles causes the permeabilities to converge. NR212 was soaked in water and electrolyte for longer times in an attempt to separate the effects of time and cycling. Resolving this discrepancy is important because it appears as though membranes approach a common set of properties once they are run in a cell. Vanadyl permeability through NR212 is presented as a function of soaking time in water and electrolyte solution in Figure 2. As-received membranes were placed in soaking solutions for various periods of time and then transferred to the permeation cell for measurement. Each point on the plots corresponds to an individual membrane sample that was discarded after a single measurement. Figure 2a shows that water imbibed the membrane rapidly. A large increase in permeability was

observed during the first several hours, followed by a slower increase over the next 3 days before reaching a plateau at 5.5×10^{-7} cm²/min. Membrane swelling in electrolyte is comparatively slower and weaker. As shown in Figure 2b, the initial large increase in permeability occurred over a period of 10 days and the slow increase lasted for 90 more days before reaching a plateau at 2.2×10^{-7} cm²/min, which is less than $\frac{1}{2}$ the permeability of the membrane in equilibrium with water. However, the selectivity in water stops changing after 3 days, and this selectivity is higher than that measured post cell testing (~ 8 days). The selectivity of membranes soaked in electrolyte continues to change over 90 days, but remains larger than both water soaked and post cell. The slow response to electrolyte contrasts strongly with the results from the charge/discharge cells. Furthermore, the selectivity of the membranes extracted from the cells is closer to the water soaked results.

Conclusions

The proton conductivities and vanadium permeabilities of reinforced Nafion XL-100, cast NR211 and NR212, and extruded N115 and N117 were measured as-received and after various pretreatments. Permeability and selectivity vary strongly with pretreatment and comparatively weakly with manufacturing process. The observed variations in selectivity substantially diminish after charge/discharge cycling in a cell and appear to converge to a single selectivity that is between the values for water-soaked and boiled membranes.

Acknowledgments

Work by Robert Darling was supported as part of the Joint Center for Energy Storage Research, an Energy Innovation Hub funded by the U.S. Department of Energy, Office of Science, Basic Energy Sciences. The authors thank their flow-battery project colleagues at UTRC. Specifically, Weina Li helped with the vanadyl concentration measurement. The work presented herein was funded, in part, by the Advanced Research Projects Agency - Energy (ARPA-E), U.S. Department of Energy (DOE) under Award Number DEAR0000149.

The information, data, or work presented herein was funded in part by an agency of the United States Government. Neither the United States Government nor any agency thereof, nor any of their employees, makes any warranty, express or implied, or assumes any legal liability or responsibility for the accuracy, completeness, or usefulness of any information, apparatus, product, or process disclosed, or represents that its use would not infringe privately owned rights. Reference herein to any specific commercial product, process, or service by trade name, trademark, manufacturer, or otherwise does not necessarily constitute or imply its endorsement, recommendation, or favoring by the United States Government or any agency thereof. The views and opinions of authors expressed herein do not necessarily state or reflect those of the United States Government or any agency thereof.

Appendix

The energy efficiency of the reactor in a flow battery is the product of the coulombic and voltage efficiencies: $\epsilon_{e,rt} = \epsilon_{q,rt}\epsilon_{v,rt}$. The subscripts e , q , v , and rt denote energy,

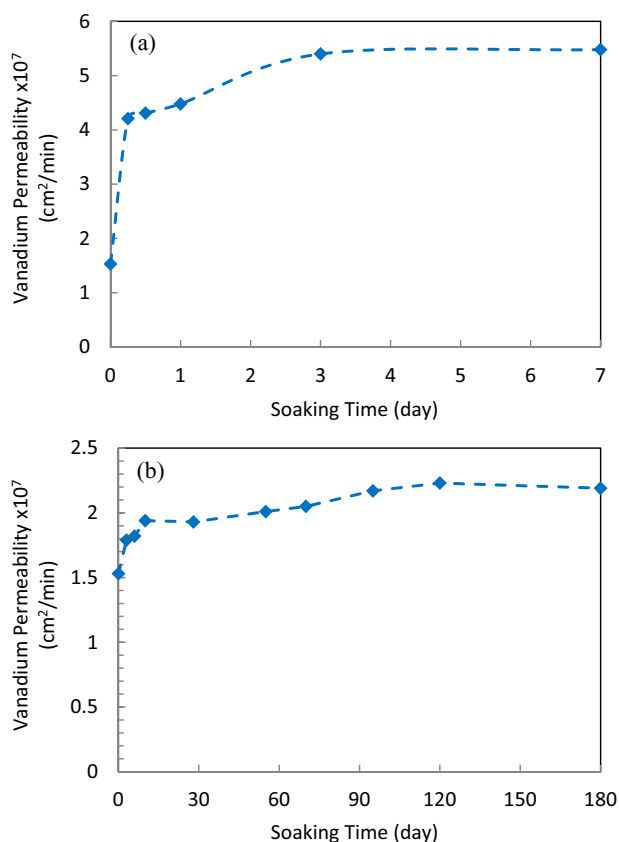


Figure 2. Vanadyl permeability as a function of time for NR212 immersed in a) water and b) electrolyte.

coulombic, voltage, and round trip, respectively. The coulombic efficiency can be approximated as:

$$\varepsilon_{q,rt} = \frac{i_d - i_x}{i_d + \tau i_x} \approx 1 - (1 + \tau) \frac{i_x}{i_d} \quad [A1]$$

The second approximation applies when the inefficiency is small. The variable i_d is the current density during discharge, i_x is the crossover current density, and τ is the ratio of charge time to discharge time. Similarly, the voltage efficiency can be approximated as:

$$\varepsilon_{v,rt} = \frac{U - i_d R_\Omega}{U + \tau^{-1} i_d R_\Omega} \approx 1 - (1 + \tau^{-1}) \frac{i_d R_\Omega}{U} \quad [A2]$$

U is the open-circuit potential and R_Ω is the area-specific resistance. $R_\Omega = R_m + R_o$, where R_o includes all sources of overpotential aside from the membrane. The current density that yields maximum efficiency can be found by differentiation:

$$\frac{\partial \varepsilon_{e,rt}}{\partial i_d} = \varepsilon_{q,rt} \frac{\partial \varepsilon_{v,rt}}{\partial i_d} + \frac{\partial \varepsilon_{q,rt}}{\partial i_d} \varepsilon_{v,rt} = 0 \quad [A3]$$

A simple analytical solution exists when the approximations for low inefficiency apply. The discharge current density that maximizes efficiency is:

$$i_d = \sqrt{\frac{(1 + \tau) i_x U}{(1 + \tau^{-1}) R_\Omega}} = \sqrt{\frac{\tau i_x U}{R_\Omega}} \quad [A4]$$

And the corresponding efficiencies are:

$$\varepsilon_{q,rt} = \varepsilon_{v,rt} = \sqrt{\varepsilon_{e,rt}} = 1 - \sqrt{(1 + \tau)(1 + \tau^{-1}) i_x R_\Omega U^{-1}} \quad [A5]$$

Interestingly, the maximum coulombic efficiency is equal to the maximum voltage efficiency. Because this paper is concerned with the membrane, R_o is set to zero and, consequently, $R_m = R_\Omega$. The product $i_x R_m$ and, consequently, the maximum energy efficiency are independent of membrane thickness provided crossover occurs by diffusion. This approximation is best at low current density, because the contribution of migration is proportional to current density. For more detail regarding competition between diffusion and migration, please refer to one of our earlier publications.²³ Conversely, the value of i_d at $\max(\varepsilon_{e,rt})$ is inversely proportional to membrane thickness. If R_o is not equal to zero, then $\max(\varepsilon_{e,rt})$ will depend on thickness.

The selectivity defined in Equation 1 can be expressed in terms of the area-specific resistance R_Ω and crossover current density i_x of the membrane:

$$\alpha = \frac{RT}{R_m i_x F}; \quad R_m = \frac{d}{\kappa}; \quad i_x = \frac{\phi F P_{ACA}}{d} \quad [A6]$$

The proportionality constant ϕ needs to be determined by an analysis of the reactions associated with crossover. For a VRFB, $\phi = 4$ if all of the crossover fluxes are equal.²³ Introducing the selectivity into the expression for the maximum efficiency yields

$$\varepsilon_{e,rt} = \left(1 - \sqrt{\frac{\phi RT (1 + \tau)(1 + \tau^{-1})}{\alpha F U}} \right)^2 \quad [A7]$$

an appealingly simple relationship between energy efficiency and selectivity.

List of Symbols

A	active membrane area in the cell, cm^2
$c_D(0)$	initial vanadyl concentration in donor chamber, M
$c_R(t)$	vanadyl concentration in receiver chamber at time t , M
d	membrane thickness, cm
F	Faraday constant, C/mol e^-
i_d	discharging current density, A cm^{-2}
i_x	crossover current density, A cm^{-2}
l	distance between the center two probes of the conductivity cell, cm
m_d	mass of dried membrane
m_h	mass of hydrated membrane
P	vanadyl permeability, cm^2/min
Q	vanadyl flux or crossover, mmol/min
R	impedance resistance, ohm
R	universal gas constant, $\text{J mol}^{-1} \text{K}^{-1}$
R_m	membrane resistance, Ωcm^{-2}
R_o	other resistance, Ωcm^{-2}
R_Ω	total resistance, Ωcm^{-2}
S	area of a membrane cross section, cm^2
t	time, min
T	temperature, K
T_g	glass transition temperature, $^\circ\text{C}$
U	open-circuit voltage, V

V volume of the solution added to each chamber of permeation cell, mL

Greek

α	selectivity of protons over vanadyl ions, dimensionless
$\varepsilon_{e,rt}$	round-trip energy efficiency, dimensionless
$\varepsilon_{q,rt}$	round-trip coulombic efficiency, dimensionless
$\varepsilon_{v,rt}$	round-trip voltage efficiency, dimensionless
ϕ	proportionality constant between crossover current and species flux
ϕ_W	volume fraction of water in hydrated membrane
κ	ionic conductivity, mS/cm
ρ_P	density of dry membrane
ρ_W	density of de-ionized water
τ	ratio of charge to discharge times, dimensionless

References

1. T. Mohammadi and M. S. Kazacos, *J. Appl. Electrochem.*, **27**(2), 153 (1997).
2. K. A. Mauritz and R. B. Moore, *Chem. Rev.*, **104**(10) (2004).
3. R. Darling, K. Gallagher, W. Xie, L. Su, and F. Brushett, *J. Electrochem. Soc.*, **163**(1) (2015).
4. S. Kim, J. Yan, B. Schwenzer, J. Zhang, L. Li, J. Liu, Z. Yang, and M. A. Hickner, *Electrochem. Commun.*, **12**(11) (2010).
5. Z. Mai, H. Zhang, X. Li, C. Bi, and H. Dai, *J. Power Sources*, **196**(1), (2011).
6. J. Qiu, L. Zhao, M. Zhai, J. Ni, H. Zhou, J. Peng, J. Li, and G. Wei, *J. Power Sources*, **177**(2) (2008).
7. D. Chen, S. Wang, M. Xiao, and Y. Meng, *J. Power Sources*, **195**(7) (2010).
8. J. Qiu, M. Li, J. Ni, M. Zhai, J. Peng, L. Xu, H. Zhou, J. Li, and G. Wei, *J. Membr. Sci.*, **297**(1–2) (2007).
9. J. Qiu, M. Zhai, J. Chen, Y. Wang, J. Peng, L. Xu, J. Li, and G. Wei, *J. Membr. Sci.*, **342**(1–2) (2009).
10. D. Chen, M. A. Hickner, E. Agar, and E. C. Kumbur, *ACS Appl. Mater. Interfaces* (2013).
11. Q. Luo, H. Zhang, J. Chen, D. You, C. Sun, and Y. Zhang, *J. Membr. Sci.*, **325**(2) (2008).
12. M. Yue, Y. Zhang, and L. Wang, *J. Appl. Polym. Sci.*, **127**(5) (2013).
13. D. Chen, M. A. Hickner, E. Agar, and E. C. Kumbur, *Electrochem. Commun.*, **26**(0) (2013).
14. DuPont Nafion Membranes. http://www2.dupont.com/FuelCells/en_US/products/nafion.html
15. W. Xie, G. M. Geise, B. D. Freeman, C. H. Lee, and J. E. McGrath, *Polymer*, **53**(7) (2012).
16. N. P. Berezina, S. V. Timofeev, and N. A. Kononenko, *J. Membr. Sci.*, **209**(2), (2002).
17. J. E. Hensley, J. D. Way, S. F. Dec, and K. D. Abney, *J. Membr. Sci.*, **298**(1–2), (2007).
18. C. E. Evans, R. D. Noble, S. Nazeri-Thompson, B. Nazeri, and C. A. Koval, *J. Membr. Sci.*, **279**(1–2) (2006).
19. W. Xie, J. Cook, H. B. Park, B. D. Freeman, C. H. Lee, and J. E. McGrath, *Polymer*, **52**(9) (2011).
20. G. M. Geise, H. B. Park, A. C. Sagle, B. D. Freeman, and J. E. McGrath, *J. Membr. Sci.*, **369** (2011).
21. B. D. Freeman, *Macromolecules*, **32**(2) (1999).
22. L. M. Robeson, B. D. Freeman, D. R. Paul, and B. W. Rowe, *J. Membr. Sci.*, **341**(1–2) (2009).
23. R. M. Darling, A. Z. Weber, M. C. Tucker, and M. L. Perry, *J. Electrochem. Soc.*, **163**(1) (2015).
24. K. Oberbroeckling, D. C. Dunwoody, and J. Leddy, In *The 198th ECS Meeting*, Phoenix, AZ, 2000.
25. X. Teng, Y. Zhao, J. Xi, Z. Wu, X. Qiu, and L. Chen, *J. Power Sources*, **189**(2) (2009).
26. A. Fick, *J. Membr. Sci.*, **100**(1) (1995).
27. R. W. Baker, *Membrane Technology and Applications*. 2nd ed., p. J. Wiley: Chichester (2004).
28. X. Teng, Y. Zhao, J. Xi, Z. Wu, X. Qiu, and L. Chen, *J. Membr. Sci.*, **341**(1–2), (2009).
29. T. A. Zawodzinski, T. E. Springer, J. Davey, R. Jestel, C. Lopez, J. Valerio, and S. Gottesfeld, *J. Electrochem. Soc.*, **140**(7) (1993).
30. Y. Shibahara, H. S. Sodaye, Y. Akiyama, S. Nishijima, Y. Honda, G. Isoyama, and S. Tagawa, *J. Power Sources*, **195**(18) (2010).
31. W. Xie, H. Ju, G. M. Geise, B. D. Freeman, J. I. Mardel, A. J. Hill, and J. E. McGrath, *Macromolecules*, **44**(11) (2011).
32. S. J. Osborn, M. K. Hassan, G. M. Divoux, D. W. Rhoades, K. A. Mauritz, and R. B. Moore, *Macromolecules*, **40**(10) (2007).
33. L. C. E. Struik, *Physical Aging in Amorphous Polymeres and Other Materials*. p. Elsevier Scientific Publishing Company: (1978).